Since January 2020 Elsevier has created a COVID-19 resource centre with free information in English and Mandarin on the novel coronavirus COVID-19. The COVID-19 resource centre is hosted on Elsevier Connect, the company's public news and information website.

Acta Biomaterialia 148 (2022) 258–270

Contents lists available at ScienceDirect

Acta Biomaterialia

journal homepage: www.elsevier.com/locate/actbio

Full length article

ROS-responsive polymer nanoparticles with enhanced loading of dexamethasone effectively modulate the lung injury microenvironment

Wali Muhammad[a,1], Jiaqi Zhu[b,1], Zihe Zhai[a], Jieqi Xie[a], Jiahang Zhou[b], Xudong Feng[b], Bing Feng[b], Qiaoling Pan[b], Shifen Li[a], Rajiu Venkatesan[a], Pan Li[b], Hongcui Cao[b,*], Changyou Gao[a,*]

[a] MOE Key Laboratory of Macromolecular Synthesis and Functionalization, Department of Polymer Science and Engineering, Zhejiang University, Hangzhou 310027, China
[b] State Key Laboratory for the Diagnosis and Treatment of Infectious Diseases, The First Affiliated Hospital, Zhejiang University School of Medicine, 79 Qingchun Rd., Hangzhou 310003, China

ARTICLE INFO

Article history:
Received 28 February 2022
Revised 9 June 2022
Accepted 10 June 2022
Available online 18 June 2022

Keywords:
Dexamethasone
ROS-responsive polymers
Nanoparticles
Acute lung injury
LPS-induced

ABSTRACT

The acute lung injury (ALI) is an inflammatory disorder associated with cytokine storm, which activates various reactive oxygen species (ROS) signaling pathways and causes severe complications in patients as currently seen in coronavirus disease 2019 (COVID-19). There is an urgent need for medication of the inflammatory lung environment and effective delivery of drugs to lung to reduce the burden of high doses of medications and attenuate inflammatory cells and pathways. Herein, we prepared dexamethasone-loaded ROS-responsive polymer nanoparticles (PFTU@DEX NPs) by a modified emulsion approach, which achieved high loading content of DEX (11.61 %). DEX was released faster from the PFTU@DEX NPs in a ROS environment, which could scavenge excessive ROS efficiently both *in vitro* and *in vivo*. The PFTU NPs and PFTU@DEX NPs showed no hemolysis and cytotoxicity. Free DEX, PFTU NPs and PFTU@DEX NPs shifted M1 macrophages to M2 macrophages in RAW264.7 cells, and showed anti-inflammatory modulation to A549 cells *in vitro*. The PFTU@DEX NPs treatment significantly reduced the increased total protein concentration in BALF of ALI mice. The delivery of PFTU@DEX NPs decreased the proportion of neutrophils significantly, mitigated the cell apoptosis remarkably compared to the other groups, reduced M1 macrophages and increased M2 macrophages *in vivo*. Moreover, the PFTU@DEX NPs had the strongest ability to suppress the expression of NLRP3, Caspase1, and IL-1β. Therefore, the PFTU@DEX NPs could efficiently suppress inflammatory cells, ROS signaling pathways, and cell apoptosis to ameliorate LPS-induced ALI.

Statement of Significance

The acute lung injury (ALI) is an inflammatory disorder associated with cytokine storm, which activates various reactive oxygen species (ROS) signaling pathways and causes severe complications in patients. There is an urgent need for medication of the inflammatory lung environment and effective delivery of drugs to modulate the inflammatory disorder and suppress the expression of ROS and inflammatory cytokines. The inhaled PFTU@DEX NPs prepared through a modified nanoemulsification method suppressed the activation of NLRP3, induced the polarization of macrophage phenotype from M1 to M2, and thereby reduced the neutrophil infiltration, inhibited the release of proteins and inflammatory mediators, and thus decreased the acute lung injury *in vivo*.

1. Introduction

The acute lung injury (ALI) is a life-threatening inflammatory disorder associated with cytokine storm syndrome, excessive levels of pro-inflammatory cytokines such as interleukins (IL), tu-

* Corresponding authors.
E-mail addresses: hccao@zju.edu.cn (H. Cao), cygao@zju.edu.cn (C. Gao).
[1] Wali Muhammad and Jiaqi Zhu contributed equally to this work

https://doi.org/10.1016/j.actbio.2022.06.024
1742-7061/

mor necrosis factors (TNF), and interferons (IFN), and can easily be developed into acute distress syndrome (ARDS) if left untreated [1–4]. The release of pro-inflammatory cytokines elicits an immune response and recruits neutrophils to the inflamed tissue, which further release noxious mediators such as reactive oxygen species (ROS) and myeloperoxidase (MPO) [5]. ROS are presumed to serve as a host defense against pathogens, and their concentration is thought to be controlled by the balance between production and scavenging [6]. The excessive formation of ROS or insufficient clearance of ROS will result in a variety of pathological diseases such as asthma, chronic obstructive pulmonary disease (COPD), and ARDS [7–9]. Endothelial cells, alveolar epithelial cells, alveolar macrophages, neutrophils, and eosinophils are among the principal ROS generators in the lung [10], which are thus linked to oxidative stress in ALI. Antioxidants have been demonstrated to lessen the severity of ALI in a variety of mice models including lipopolysaccharide (LPS)-induced ALI [10–12]. Recent studies have proved that the seriousness of COVID-19 is also associated with an increase in ROS formation [13–15]. When the severe acute respiratory syndrome- coronavirus-2 (SARS-CoV-2) enters the airways, the immune response begins upon the virus replication. The activation of macrophages and dendritic cells via the Toll-like NOD receptors initiates the immunological innate response against the generation of inflammatory cytokines and ROS. Activated macrophages and neutrophils release superoxide radicals and H_2O_2, causing oxidative stress [15]. Therefore, blocking the excessive level of ROS to alleviate oxidative stress is a promising strategy to lessen lung inflammation.

A range of ROS-responsive materials, such as scaffolds, hydrogels, and nanoparticles (NPs), have recently been settled to respond to physiological oxidative microenvironments [16,17]. To specifically target inflamed lung tissues, ROS-responsive NPs have been developed to deliver therapeutic drugs that modulate the ALI microenvironment [5,18,19]. For example, a ROS-responsive material 4-(hydroxymethyl phenylboronic acid pinacol ester)-modified cyclodextrin was employed as a carrier to encapsulate moxifloxacin to create a core-shell NPs, whose surface was further coated with 2-distearoyl-sn-glycer-3-pho-sphoethanolamine-polyethylene glycol folic acid [20]. The ROS-responsive NPs smartly target macrophages and release antibiotics in an excessive ROS environment. Moreover, an immunosuppressant (FK-506) was loaded into ROS-responsive NPs prepared from poly(1,4-phenleneacetonedimethylene thioketal) [21]. These NPs significantly suppress the release of pro-inflammatory cytokines and diminish the inflammation caused by PM 2.5 particulates *in vivo*.

One of the main critical issues in NPs synthesis is the low drug loading amount. The majority of nanomedicines have a low drug loading, leading to clinical translation challenges due to obstacles such as high production cost, scaling-up products with repeatable qualities, and possible toxic side effects [22]. In polymeric NPs, the drug loading content less than 10% is considered to hinder the practical applicability [23]. Previously, high drug loading (>50%) to polymeric NPs showed significant stability in physiological conditions [24]. Additionally, several drugs such as camptothecin, ciprofloxacin, curcumin, λ-cyhalothrin, and paclitaxel and polymers pluronic F127, dextran sulfate, poly(lactide)-poly (ethylene glycol) (PLA-PEG), and poly(N-vinyl pyrolidone)-b-poly(ε-caprolactone) have been employed to produce NPs with drug loading ranging from 20 to 80% [22,25-28]. Moreover, achieving a pharmacological therapeutic window necessitates a very high concentration of NPs that sometimes makes endotracheal delivery challenging because of viscous solution. Therefore, it is critical to increase the drug loading content into NPs to avoid such complications.

To achieve high drug loading into NPs and target lung inflamed tissue, a novel strategy should be applied to minimize the use of high doses of medications and high levels of ROS formation to alleviate lung injury. Herein, inspired by the sequential nanoprecipitation method [23], a modified-emulsion is developed to maximize drug loading into NPs. The polyurethane (PFTU) synthesized by our group [29] containing ROS-responsive thioketal bonds in the main chain is used to prepare the dexamethasone (DEX)-loaded ROS-responsive NPs. The fibrous film prepared by PFTU displays good antioxidant and ROS-responsive degradation *in vitro*. DEX can inhibit the intensive inflammation reaction caused by LPS-induced lung injury [30]. In addition, DEX suppresses the level of pro-inflammatory cytokines, chemokines, and myeloperoxidase (MPO) activity, and reduces the expressions of COX-2, iNOS, and NF-κB p65 in the LPS-induced ALI model [31]. The loaded DEX can be released faster in a ROS excessive environment (Scheme 1), which, together with the NPs matrix, modulates the lung injury microenvironment significantly.

2. Materials and methods

2.1. Materials

The following materials and chemicals were used in the current experiment: A549 cells obtained from the cell bank of typical culture collection of the Chinese Academy of Sciences (Shanghai, China), dexamethasone-17-acetate (DEX, > 98%, Aladdin Co. Ltd), lipopolysaccharide (LPS) (Sigma-Aldrich), Roswell Park Memorial Institute-RPMI 1640 (Life Technology Cooperation's, USA), Dulbecco's modified Eagle medium (DMEM, Gibco, USA), 2,2-diphenyl-1-picrylhydrazyl-DPPH (Aladdin Chemistry Co., Ltd., China), trichloromethane ($CHCl_3$, grade, analytical reagent (AR), methanol (grade, AR), acetone (grade, AR) and dimethyl sulfoxide (DMSO, grade, AR) (Sinopharm Chemical Reagent Company, China), enzyme-linked immunosorbent assay (ELISA) kit for TNF-α, IL-1β and IL-6 (BosterBio, Wuhan, China), ELISA kit for IL-4 and IL-10 (Elabscience Biotechnology), Lactate dehydrogenase (LDH) cytotoxicity assay kit (Beyotime, Biotechnology, China), TUNEL BrightGreen Apoptosis Detection Kit (A112-02, Vazyme, Nanjing, China), and 4,5-dimethylthiazol-2-yl)-2,5-diphenyl-2H-tetrazolium bromide (MTT) (Sigma-Aldrich).

2.2. Preparation of NPs

A ROS-responsive polyurethane (PFTU) synthesized in our lab [29] from poly(propylene fumarate) (PPF), poly(thioketal) (PTK) and a 1,6-hexamethylene diisocyanate (HDI) and further chain-extended with a ROS-cleavable thioketal diamine was used as the key materials to prepare the DEX-loaded NPs (PFTU@DEX NPs).

The PFTU@DEX NPs were prepared by a modified emulsification method. In brief, the PFTU (2%) was dissolved in trichloromethane ($CHCl_3$), and DEX (10 mg) was dissolved in a mixture of three solvents (methanol, acetone, and DMSO) with 1:1:1 ratio in volume (total volume 0.9 mL). 1 mL PFTU solution was then added to the DEX solution to obtain the PFTU@DEX NPs mixture, which was further added into a PVA solution (2% w/v). After the mixture was dispersed by a probe sonicator (amplitude 40%, Sonicator 4000, Misonix, U.S.A., probe tip diameter: 3.2 mm) for 1 min under an ice bath, the suspension was quickly poured into distilled water (30 mL). A same volume of phosphate buffered saline (PBS, pH 7.4) was added after 5 min, before the mixture was magnetically stirred for 6 h at room temperature. The obtained NPs were centrifuged (12000 rpm, 10 min), followed by washing with Milli-Q water (3 times), and finally re-suspended with deionized water. The blank NPs (PFTU NPs) were also prepared with the same method without the addition of DEX.

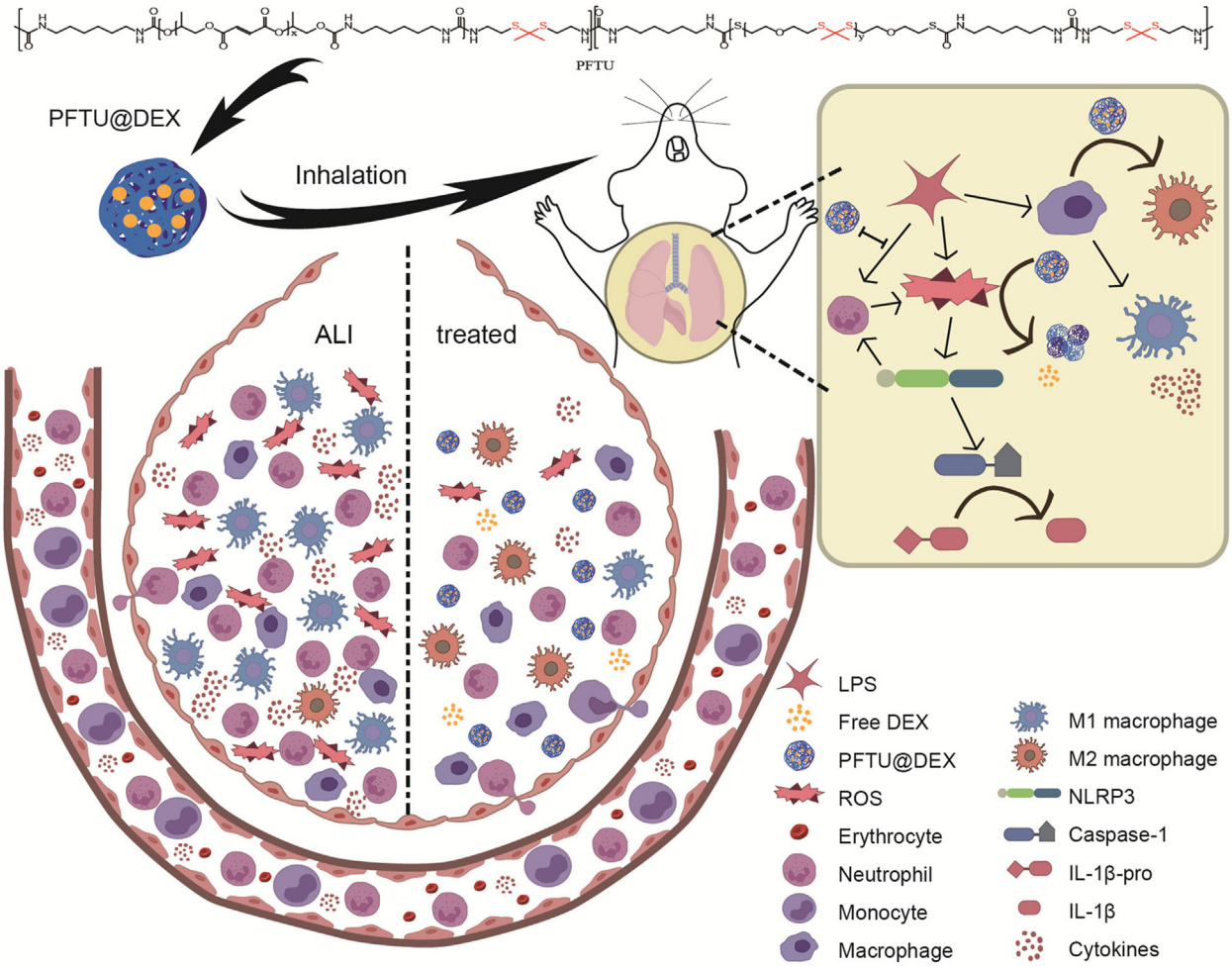

Scheme 1. Schematic illustration of the ROS-responsive polymer (PFTU) used for the preparation of PFTU@DEX NPs through a modified emulsion method, which are delivered to the lung through endotracheal intubation atomization. The DEX is released faster when being exposed to excessive ROS, which in turn modulates LPS-induced acute lung injury microenvironment and better therapy for acute lung injury.

2.3. Characterization of PFTU NPs and PFTU@DEX NPs

The particle size and polydispersity index (PDI) of PFTU@DEX NPs and PFTU NPs were determined by dynamic light scattering (DLS, Delsa Nano C, Beckman Coulter). The morphology of both NPs was characterized by scanning electron microscopy (SEM, SEM, S-4800, Hitachi). To assess the stability of PFTU NPs and PFTU@DEX NPs, the synthesized NPs solution was kept in a vial at room temperature, and their size and PDI were measured by DLS along with time prolongation until 30 d.

The DEX loading content in the PFTU@DEX NPs was quantified by high-performance liquid chromatography (HPLC). In brief, the PFTU@DEX NPs were lyophilized, weighed, and re-dispersed in methanol. After ultrasonication, the NPs were centrifuged to collect the supernatant, which was subjected to HPLC (HPLC-515, Waters) equipped with an Agilent Zorbax RX-C 18 column and a diode-array UV detector (254 nm). The DEX amount was quantified according to the standard curve of DEX. The following equation was used to calculate the DEX loading content in NPs.

$$\text{LC\%} = \text{Amount of DEX in NPs}/\text{Total weight of NPs} \times 100$$

The *in vitro* drug release experiment was conducted in PBS and ROS environment (1 mM H_2O_2). The freeze-dried PFTU@DEX NPs were sealed in a dialysis bag, and were kept in a beaker containing 50 mL PBS or H_2O_2. The beaker was maintained at 37 °C with gentle shaking. 1 mL solution was collected at different time intervals, and the same volume of medium was supplemented to keep the total volume constant. The concentration of DEX in the medium was measured by HPLC.

2.4. In vitro experiments

2.4.1. Antioxidant activity of NPs

To evaluate the antioxidant activity of NPs, a 2,2-diphenyl-1-picrylhydrazyl (DPPH, molar mass, 394.32 g/mol) scavenging assay was used. The DPPH solution (200 μM) was prepared in ethanol, in which different concentrations of DEX and NPs (100-1000 μg/mL) were incubated for 2 h under 37 °C. The antioxidant capacity was assessed by measuring the absorbance at 517 nm using a microplate reader (Infinite M200 Pro, Tecan). DPPH solution was used as a control. The following formula was used to express the antioxidant capacity in percentage,

$$\%\text{inhibition} = (\text{AB} - \text{AS})/\text{AB} \times 100,$$

where AB is the DPPH (control) absorbance, and AS is the absorbance of the sample (DPPH + sample).

2.4.2. Cytotoxicity of DEX, PFTU NPs and PFTU@DEX NPs

The cell viability of drug and NPs was checked by an MTT assay. A549 (lung carcinoma epithelial) cells were cultured in Roswell

Park Memorial Institute (RPMI) 1640 medium, and RAW 264.7 murine macrophages were cultured in high-glucose DMEM containing 100 U/mL penicillin, 100 μg/mL streptomycin, and 10% fetal bovine serum (FBS). The A549 and RAW264.7 cells were seeded in 96 well plates at a density of 5×10^3 and 1×10^4 cells/well, respectively, and maintained in an incubator (Thermo Scientific, 37 °C, 5% CO_2). The original culture mediums were replaced with a fresh one (100 μL) containing different concentrations of DEX and NPs (25-1000 μg/mL). After 48 h, 10 μL MTT was added to each well, which was then further incubated for 4 h. After the formazan crystals were dissolved by DMSO, the absorbance was measured at 570 nm.

Biocompatibility of NPs with red blood cells (RBCs) was also evaluated by a hemolysis assay [32]. The fresh blood (FB) was collected from rats in ethylenediamine tetraacetic acid (EDTA) tubes. To isolate the erythrocytes, the FB was centrifuged at 1500 rpm for 5 min to obtain pellets, which were washed 3 times and diluted with PBS finally. The diluted suspension (200 μL) was incubated with 800 μL of PBS containing several concentrations of NPs (1 h, 37°C). The RBCs incubated with water and PBS were used as a positive and negative control, respectively. Centrifugation (2500 rpm, 5min) was performed to separate supernatant, whose absorbance was measured at 545 nm by a microplate reader.

2.4.3. Analysis of cytokines by ELISA

Enzyme-linked immunosorbent assay (ELISA) was used to quantify the secretion of cytokines in lipopolysaccharides (LPS)-stimulated A549 and RAW264.7 cells. In brief, A549 and RAW264.7 cells were seeded in 96-well plates according to the above protocols, which were later plated in 12-well plates. The cells were pretreated with or without DEX, PFTU NPs, and PFTU@DEX NPs. One hour later, A549 and RAW264.7 cells were stimulated by LPS (1 μg/mL) and then maintained for 24 h at 37°C. The supernatant was collected by centrifugation (3,000 rpm, 30 min) after 24 h, and was tested for TNF-α, IL-1β, IL-6 (pro-inflammatory), IL-4 and IL-10 (anti-inflammatory) levels by using ELISA kits according to the manufactures' instructions.

2.5. In vivo experiments

2.5.1. Mouse ALI model

The ALI model was established by endotracheal intubation atomization of healthy wild-type (WT) C57 male 6-8w mice (18-22g) with 20 μg/g LPS. The mice were purchased from Shanghai Slake Laboratory Animal Co., Ltd, Shanghai, China. After 4 h, the LPS, DEX, PFTU NPs and groups were administered with 35 μL double distilled water (ddH_2O, 35 μL DEX solution (ultrasonically dispersed in ddH_2O after dissolved by 1/1000 DMSO, 1.2 mg/kg), 35 μL PFTU NPs solution (ddH_2O dispersion, 6.4 mg/mL), and 35 μL PFTU@DEX NPs solution (ddH_2O dispersion, 6.4 mg/mL, equal to 1.2 mg/kg of free DEX), respectively. The healthy group received the same treatment, but PBS was used instead of LPS and ddH_2O was used instead of NPs. All the above-mentioned drugs were administered by endotracheal intubation and atomization through a microsprayer aerosolizer (BJ-PW-M, BioJane, China), once every 24 h, for three times in total, and the samples were taken for analysis at 72 h, which is the time point of acute lung injury [33–35]. These group settings were used for the subsequent experiments unless otherwise stated. One hundred and fifteen mice were randomly divided into five groups: PBS group, LPS group, DEX group, PFTU NPs group, and PFTU@DEX NPs group (n = 21-24). At the time point, 5 mice in each group were euthanized, and the tissues were fixed in 4% paraformaldehyde for pathological analysis. For bronchoalveolar lavage fluid analysis of lung tissues, 3 to 5 mice were analyzed for each group. The other 4 mice per group were analyzed for ROS expression *in vivo*, and 4 for Western blot analysis. Lung immune cell isolation and macrophage flow cytometry were performed in a separate 5 mice per group. All experiments were conducted using protocols approved by the Animal Care Ethics Committee of the First Affiliated Hospital, Zhejiang University. The euthanasia method was cervical dislocation when needed.

2.5.2. HE staining of lung tissue pathology and injury score analysis

Fresh lung tissues were harvested and fixed with 4% paraformaldehyde for more than 24 h, and then embedded in paraffin and sectionalized. Each section was 5 μm thick, and was stained with hematoxylin eosin following the standard protocol. The areas of specific concern were analyzed after sealing by NanoZoomer 2.0-RS scanner (Hamamatsu, Shizuoka, Japan). The lung injury score was measured as previously described [36]. Briefly, according to the four independent indicators: pulmonary hemorrhage, neutrophils infiltration, congestion in the pulmonary capillary, and septal thickening, the severity of the lung injury was graded from 0 to 4: 0, normal; 1, mild damage (< 25% injury of the field); 2, moderate damage (25% to 50% injury of the field); 3, severe damage (50% to 75% injury of the field); and 4, extremely severe damage (> 75% injury of the field). The score of each mouse was calculated as the mean of five randomly select fields.

2.5.3. Extraction and detection of bronchoalveolar lavage fluid (BALF)

After dissecting the mice, the trachea and lungs were exposed. After a trocar was inserted into the trachea, its needle was removed. The remaining hose was connected to a 1 mL syringe containing 800 μL PBS. Repeated suction was performed three times to recover the alveolar lavage fluid and cells, with more than 650 μL of liquid being recovered in each time. After centrifuged at 400 g for 5 min, the supernatant of the first suction was collected and frozen at -80 °C for detection of BALF protein concentration by a BCA Protein Assay Kit (Biyuntian) and inflammatory factor concentrations. The cell precipitates of all the suction medium were merged, in which the red blood cells were lysed by ACK lysing buffer (GBA1049201; corning). The cell precipitation was then divided into two parts. One part of the cells was used to count the total number of cells in the alveolar lavage fluid by a cell counting plate, and the other part cells were stained and analyzed by flow cytometry. The obtained cells were stained for FVS780 (565388; BD), CD11b (562950; BD), and Ly6G (127607; Biolegend) successively. CD11b and Ly6G were used to identify neutrophils. Data were acquired via CytoFLEX LX Flow Cytometer (Beckman Coulter, Inc.).

2.5.4. Detection of BALF and serum inflammatory factors

The whole blood of each experimental mouse was taken into a procoagulant tube, and the serum was centrifuged at 3000 rpm for 15 min after being stored for 1 to 2 h. The serum was separated, packed, and frozen at -80 °C for subsequent experiments. The freezable alveolar lavage fluid supernatant and serum were tested with commercial kits for inflammatory factor concentrations by flow cytometry (LEGENDplexTM Multi-Analyte Flow Assay Kit; Biolegend). Data were acquired via CytoFLEX LX Flow Cytometer (Beckman Coulter, Inc.).

2.5.5. Immunohistochemistry of MPO and TUNEL analysis

Fresh lung tissues were harvested and fixed with 4% paraformaldehyde for more than 24 h, and then embedded in paraffin and sliced into 5-μm thick sections. The process of immunohistochemical staining for each section was the same as the normal immunohistochemistry steps. The primary antibody was MPO polyclonal antibody (PA5-16672; Invitrogen). TUNEL staining was performed on each section by a TUNEL BrightGreen Apoptosis Detection Kit (A112-02, Vazyme, Nanjing, China) according to the manufacturer's instructions.

2.5.6. Detection of ROS expression in vivo

The L-012 probe (143556-24-5, Wako Chemical) was ultrasonically dissolved with sterile PBS and stored away from light. The mice were anesthetized with 4% chloral hydrate (200 μL per 20 g mice. Sangon Biotech). The hair was removed to avoid influence on imaging. After the control shot of each mouse, the L-012 probe (50 μg/g) was injected via the mouse tail vein. The luminescence images were captured by IVIS (LuminaLT, PerkinElmer). After 40 min of L-012 injection, the lung tissues of the mice were dissected and harvested, which were imaged to detect the ROS concentration.

2.5.7. Isolation of lung immune cells and flow cytometry of pulmonary macrophages

After the experimental mice were anesthetized by 4% chloral hydrate (200 μL per 20 g mice), PBS was used to perfuse the heart until pale. After the lung tissue was separated, an enzyme mixture (The mouse Lung Dissociation Kit from Miltenyi Biotec, Bergisch Gladbach, Germany) was used for digestion and dissociation to obtain single-cell suspension through the guidance of the mouse Lung Dissociation Kit (Miltenyi Biotec, Bergisch Gladbach, Germany). Immune cells were obtained after density gradient centrifugation purification, and the red blood cells were lysed by ACK lysing buffer (GBA1049201; corning). Finally, the immune cells in lung tissue were obtained by PBS cleaning, and used for flow cytometry after staining.

FVS780 (565388; BD) was used as a dye to identify the live cells, and Fc blocker (553141; BD) was used to avoid non-specific staining. CD45 (553079; BD) was used to identify immune cells, and CD11b (562950; BD) and F4/80 (565410; BD) were used to identify macrophages. After the surface marker staining, the cells were fixed with a fixative solution (88-8824-00; BD). The membrane breaking solution was used for membrane breaking perforation, and then intracellular indicators iNOS (17-5920-82; ebiocsience) and Arg-1 (48-3697-82; ebiocsience) were stained. iNOS was used as an indicator of M1, and Arg-1 was used as an indicator of M2. Data were acquired via CytoFLEX LX Flow Cytometer (Beckman Coulter, Inc.).

2.5.8. Western blot analysis

Protein samples were harvested from fresh lung tissue using a RIPA lysis buffer (Beyotime Biotech Co., Ltd., Shanghai, China) mixed with phosphatase inhibitor cocktail and protease inhibitor cocktail (Sigma Aldrich). The protein concentration was determined by the BCA Protein Assay Kit (P0012S; Beyotime). A total of 20-30 μg protein per sample was run on 12% SDS-PAGE, and then transferred onto a nitrocellulose membrane. Subsequently, the membranes were incubated with QuickBlock Blocking Buffer (Beyotime Biotech Co., Ltd.) at room temperature for 1 h, followed by incubation with a specific primary antibody at 4 °C overnight. The primary antibody included Rabbit monoclonal [EPR23094-1] to NLRP3 (1:1000; ab263899; Abcam), caspase 1/p20/p10 polyclonal antibody (1:1000; 22915-1-AP; Proteintech), IL-1β (3A6) Mouse mAb (1:1000; 12242; Cell signaling) and beta tubulin polyclonal antibody (1:1000; 10094-1-AP; Proteintech). After washed twice, the membranes were incubated with specific secondary antibodies, including horseradish peroxidase-conjugated goat anti-rabbit IgG (1:2000; ab6721; Abcam) and horseradish peroxidase-conjugated rabbit anti-mouse IgG (1:2000; ab6728; Abcam) for 1 h at room temperature. The membranes were incubated with SuperSignal™ West Pico PLUS Chemiluminescent Substrate (34577; ThermoFisher) and detected by the ChemiScope Western Blot Imaging System (Clinx Science Instruments Co., Ltd., Shanghai, China). ImageJ software (NIH, Bethesda, MD, United States) was used to analyze the image.

2.6. Statistical analysis

Data are presented as means ± standard deviation (SD). Statistical significance among multiple groups was analyzed using the one-way analysis of variance (ANOVA) with a Tukey post hoc test. Data analysis was conducted using GraphPad Prism 8.0.1 (GraphPad Software Inc., La Jolla, CA, USA). Difference was considered statistically significant when the P-value was < 0.05, unless otherwise noted.

3. Results and discussion

3.1. Preparation and characterization of PFTU@DEX NPs

The ROS-responsive polymer synthesized from PPF, PTK and HDI was used to prepare the PFTU NPs and PFTU@DEX NPs. Herein, the PFTU@DEX NPs were prepared via a modified nanoemulsion method. The drug loading to NPs is mainly influenced by the solubility of drugs in medium [37,38]. The more soluble the drug is, the more content will be loaded to NPs. To achieve the maximum intrinsic solubility of DEX, a mixture of solvents (methanol, acetone, and DMSO) was used with 1:1:1 volume ratio. The mixture was then emulsified with PFTU containing PVA and poured into water, followed by addition of PBS. The largest DEX loaded was 11.61% in the obtained NPs (Table S1), which was almost doubled compared to the traditional method by using a single solvent (6.62% Table S1). The high loading content of DEX reveals that multiple solvents offer a strong solute-solvent attraction. During the preparation of PFTU@DEX NPs, PBS (7.4 pH) was added to the solution, which played a foremost role in controlling the inner environment pH and encapsulation efficiency [23]. It has been considered that loading of drugs to polymer NPs less than 10% may present obstacles during administration [23]. In our study, more than 10% drug loading was achieved. Moreover, NPs prepared by this approach may decrease the burden of high doses of medication to minimize complications [37], and can reduce the utilization of materials, offering the cost-effective advantage and reduced side effects [23].

The modified emulsion method not only increases the DEX loading content but also tune the size of NPs. The average size of PFTU NPs and PFTU@DEX NPs were 167±6 and 251±3 (Table S1) respectively, measured by DLS. These NPs' sizes were found smaller compared to the NPs prepared via the conventional method (Table S1). The relatively smaller size may be tired with the difference in solvent evaporation and thereby the solidation of NPs. An increase in the concentration of PVA (2% w/v) compared to the conventional one (1% w/v) may take an important role too.

The morphologies of the PFTU NPs and PFTU@DEX NPs were examined by SEM. The samples were put on a glass slide, dried overnight at room temperature and gold sputtered before detection. SEM images indicate that the PFTU NPs and PFTU@DEX NPs possessed a spherical morphology with relatively narrow distribution (Fig. 1A), confirming the successful fabrication.

The colloidal stability of NPs was evaluated by measuring the NPs size and polydispersity index (PDI) by DLS as a function of time. The NPs size was almost stable up to 30 d, but the PDI increased to some extent 10 d and 30 d later for the PFTU NPs and PFTU@DEX NPs (Fig. 1B), respectively. Therefore, the preparation approach is rapid, simple, and efficient for modification of PFTU@DEX NPs, and may be applied for preparation of various types of NPs with a high drug loading content too. Meanwhile, the up and down ratio of various factors (solvents, drugs, polymers, and PBS) may give a new direction for further optimization.

The *in vitro* drug release profile of DEX was measured in PBS (pH 7.4) and H_2O_2 (1 mM). This concentration (1 mM, H_2O_2) is selected based on the ROS level of inflammatory microenvironment and macrophage activation. The normal human plasma contains

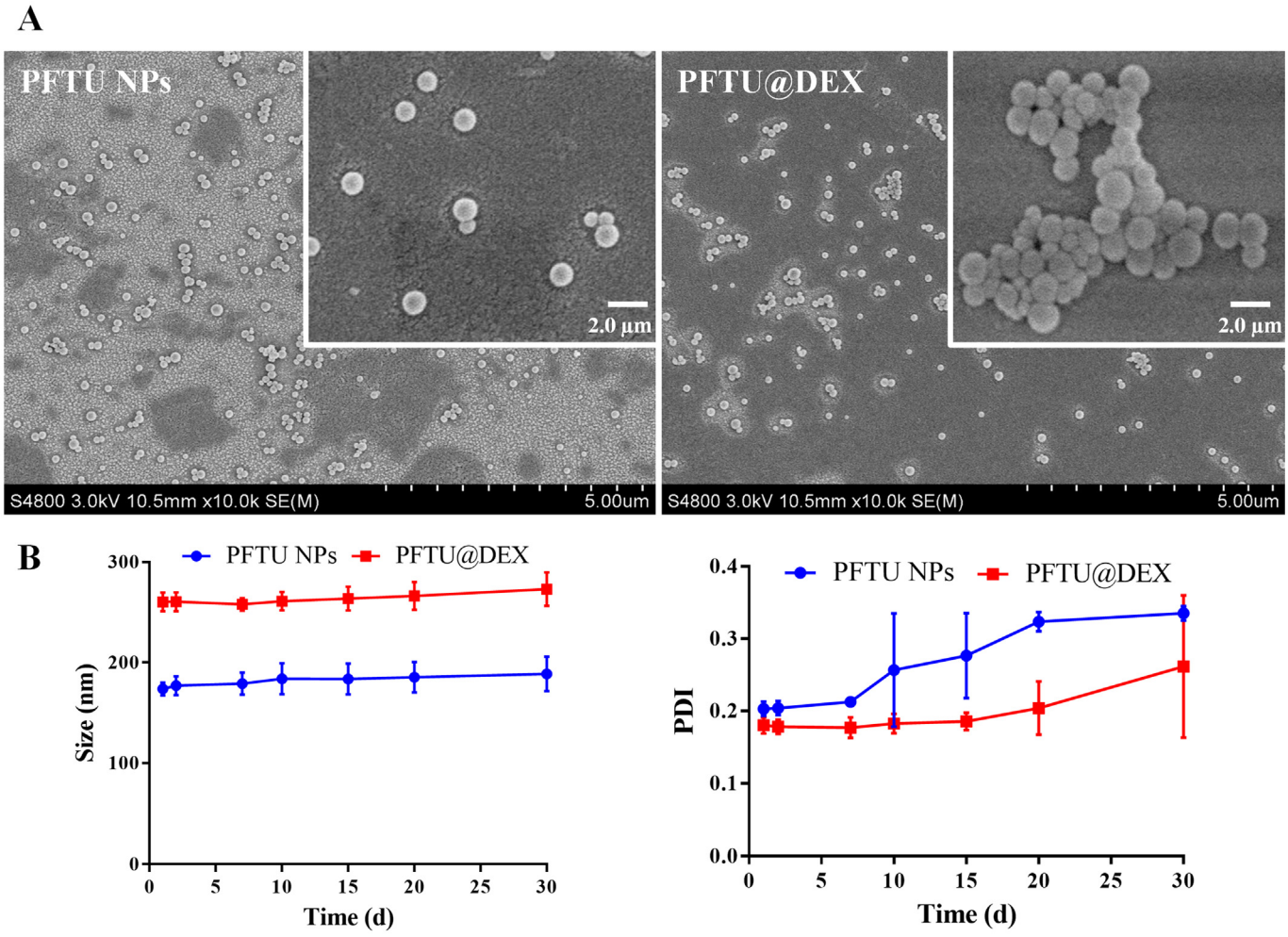

Fig. 1. (A) SEM images of PFTU NPs and PFTU@DEX NPs showing a spherical morphology. (B) Size and PDI of PFTU NPs and PFTU@DEX NPs being stored in aqueous solution along with time prolongation.

1-8 μM H_2O_2 while healthy cells generate only 1 μM ROS as a result of metabolism. The inflammatory microenvironment has a high level of ROS (10–1000 μM), and the macrophages can generate 6×10^{-14} mol H_2O_2 per h per cell [16]. More than 90% of DEX was released in 1 mM H_2O_2 from the PFTU@DEX NPs, whereas only 55% of DEX was released without H_2O_2 at the same time (Fig. 2D). The accelerated release of DEX in oxidative H_2O_2 is attributed to the ROS-responsive moiety, thioketal [39]. Thioketal groups are one of the most effective ROS-responsive chemical structures that can easily be cleaved by ROS. Owing to this quality they have been used in several studies to create ROS-responsive carrier systems for control drug release [40]. The thioketal bonds in PFTU polymers can be cleaved when expose to H_2O_2 solution, which accelerate its degradation and in turn the release of DEX.

To evaluate the potential cytotoxicity of DEX, PFTU NPs and PFTU@DEX NPs, a viability assay of A549 cells were carried out. The MTT assay exhibited that the cell viability of DEX and NPs with various concentrations had no obvious difference (Fig. 2A). Macrophages are thought to be important in the progression of ALI. Macrophages in the alveoli are the first defenders activated by infection, and thus play a key role in the initiation and maintenance of inflammatory response [5]. Here, RAW264.7 cells were used to mimic alveolar macrophages, whose viability was examined after incubation with various concentrations of DEX and NPs. The cell viability was inhibited by free DEX in RAW264.7 cells, while no obvious inhibition was found by the PFTU NPs and PFTU@DEX NPs (Fig. 2B), which is consistent with previous finding that ROS-responsive polymer NPs (PTKNPs) loaded with DEX have no notable toxicity to RAW264.7 cells [41]. These experimental data suggest that the PFTU NPs, as a carrier, might protect cells against drug toxicity and prevent cells from being exposed to excessive drug concentrations. Moreover, the LDH release data disclose that the effects of DEX, PFTU NPs and PFTU@DEX effect were dose-dependent towards RAW264.7 cells (Fig. S2).

Hemolysis occurs when RBCs are damaged, causing the iron-containing protein “hemoglobin” to be released into the plasma [42]. Here, we assessed the hemolytic activity of DEX, PFTU NPs, and PFTU@DEX NPs to confirm whether the drug or NPs cause destruction to RBCs or not. For this purpose, different concentrations of NPs and DEX were incubated with erythrocytes. The overall results show that the hemolysis was less than 5% (Fig. S3), suggesting non-hemolysis of these materials according to the national biosafety standards [43,44].

3.2. Intrinsic antioxidant activity and mediation of cytokine levels in vitro

Antioxidant compounds combined with biological materials could provide local antioxidant therapy to reduce oxidative stress-related pathologies [45]. DPPH assay, which is considered one of the standard tests for the biomaterial’s antioxidant capacity, was used to assess the NPs antioxidant activity [46]. The antioxida-

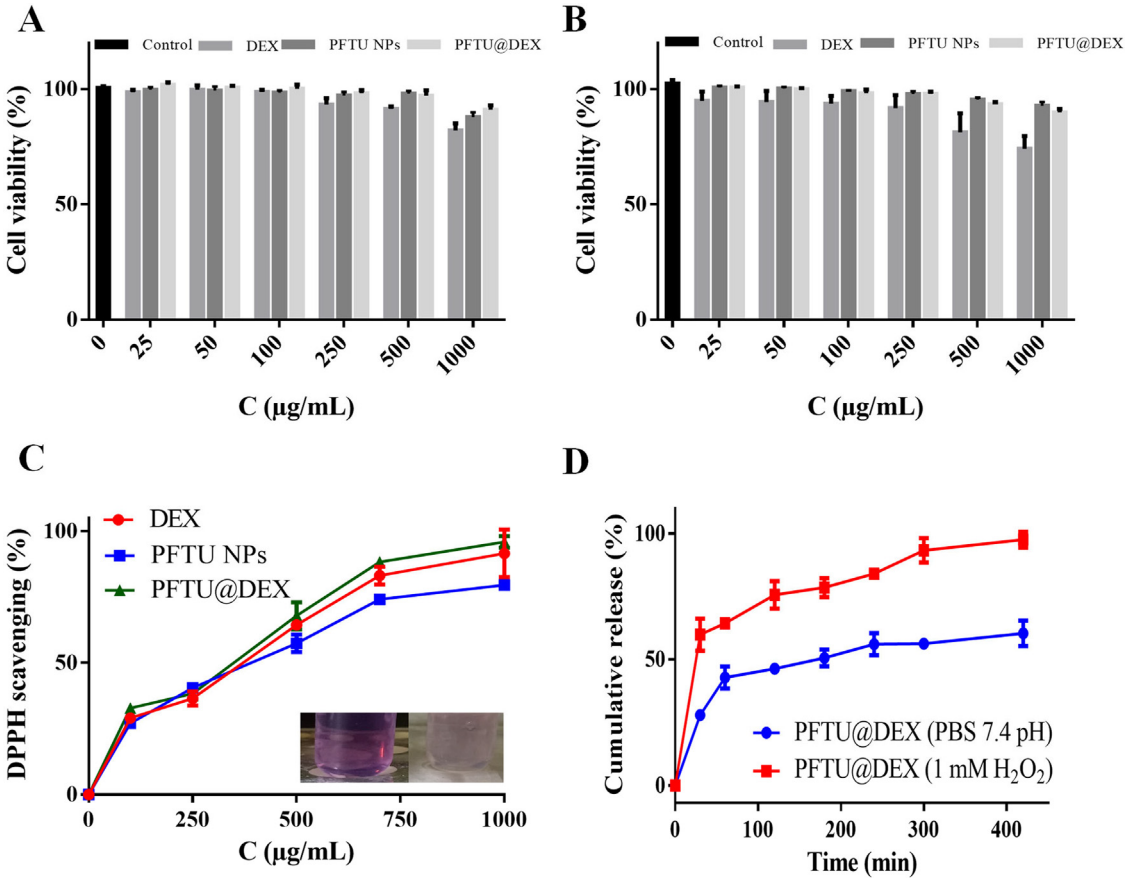

Fig. 2. (A) Viability of A549 cells being incubated with DEX, PFTU NPs and PFTU@DEX NPs for 48 h (n=5). (B) Viability of RAW264.7 cells being incubated with DEX, PFTU NPs and PFTU@DEX NPs for 48 h (n=5). (C) DPPH assay of inhibition of free radicals by DEX, PFTU NPs and PFTU@DEX NPs (100-1000 μg/mL) for 2 h at 37 °C (n=3). (D) Cumulative release of DEX from NPs in PBS (7.4 pH) and H_2O_2 (1 mM).

tion activity was evaluated for DEX, PFTU NPs, and PFTU@DEX NPs, which successfully scavenged the DPPH radicals. Fig. 2C shows that the amount of scavenging increased along with the concentration of DEX, PFTU NPs, and PFTU@DEX NPs. The higher scavenging capacity of the PFTU NPs is mainly attributed to the dense thioketal moieties in the polymer backbone [39]. The enhanced antioxidation ability of the PFTU@DEX NPs suggests that the released DEX takes a synergistic role as well.

The ability of macrophage polarization is critical for tissue repair and hemostasis maintenance in response to specific microenvironmental stimuli and signals [47]. The LPS-stimulated macrophages are polarized to the pro-inflammatory M1 phenotype secreting pro-inflammatory cytokines such as TNF-α, IL-1β and IL-6, which are critical in the onset and progression of inflammation in ALI [41]. The levels of pro-inflammatory TNF-α, IL-1β, and IL-6 were determined in RAW264.7 cells after being stimulated by LPS. The cells exhibited a high level of cytokine secretion after 24 h, which was attenuated to some extent by the free DEX and PFTU NPs, and significantly by the PFTU@DEX NPs, suggesting the strongest polarization of macrophages from M1 to M2 (Fig. 3A-C). On the other hand, the PFTU@DEX NPs significantly increased the secretion of anti-inflammatory cytokines IL-4 and IL-10, and showed notable repolarization of macrophage into M2 phenotype by upregulating these cytokine levels (Fig. S4A,B).

The levels of these pro-inflammatory cytokines were also quantified in A549 cells being stimulated by LPS. The levels of cytokine secretion were at peak upon stimulation of LPS, which were significantly reduced by free DEX-treated cells (Fig. 3D-F) as observed before [48]. The PFTU NPs had a substantial effect on reducing the cytokine level as well, and the PFTU@DEX NPs showed the strongest ability to suppress the level of IL-6 (Fig. 3F). These results indicate that the ROS-responsive NPs with the addition of DEX synergistically play a critical role in the polarization of macrophages from M1 to M2 and also help reduce inflammation *in vitro*.

3.3. PFTU@DEX NPs ameliorated LPS-induced ALI in vivo

Next, the free DEX, PFTU NPs, and PFTU@DEX NPs were used to treat ALI *in vivo*, which is one of the typical diseases involved in severe inflammatory cytokine storm and overproduction of ROS [49]. To determine how the PFTU@DEX NPs ameliorate LPS-induced ALI, the mice were divided into five groups: PBS group, LPS group, DEX group, PFTU NPs group, and PFTU@DEX NPs group. Inhalation delivery is becoming more attractive for the treatment of lung inflammatory diseases because of the possibility of targeted treatment in the lung with high medication concentration at the site of illness. Local targeting and reduced systemic exposure may lessen the occurrence of unfavorable side effects associated with systemic treatment of anti-inflammatory agents such as glucocorticoids, although the quick absorption across the pulmonary epithelium's highly absorptive surface may restrict the efficacy of targeted treatment to some extent. Therefore, the inhalation of medicines contained in a polymeric matrix has been extensively studied as a potential method of overcoming the short residence time and low lung drug concentration [50]. The benefits of employing nanotechnology for drug administration via inhalation route include targeted drug delivery, higher effectiveness, lower toxicity, reduced biodistribution, enhanced bioavailability and im-

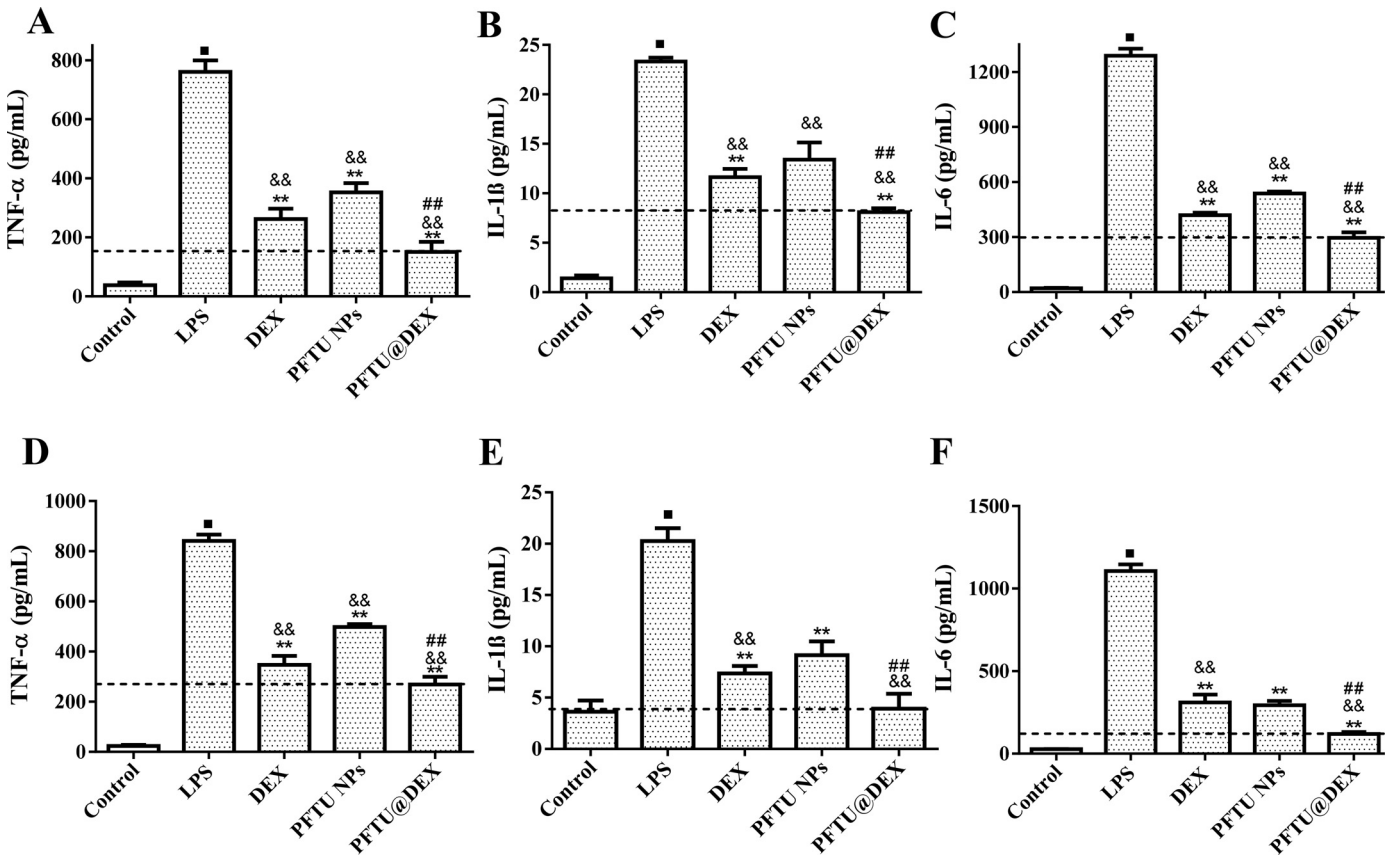

Fig. 3. Expression of (A, D) TNF-α, (B, E) IL-1β and (C, F) IL-6 in (A-C) RAW264.7 and (D-F) A549 cells being stimulated by LPS for 24 h at 37 °C and treated with different materials (n=4). The dotted horizontal line represents the mean of PFTU@DEX NPs group. ANOVA followed by Tukey-test. Data are expressed as mean ± SD $^{**}P < 0.01$ vs LPS group. $^{\&\&}P < 0.01$ vs DEX group. $^{\#\#}P < 0.01$ vs PFTU NPs group.

proved patient comfort [5,51]. Modeling and drug administration were improved by endotracheal intubation atomization (Fig. S1). Trypan Blue was delivered along the trachea, which achieved disperse distribution successfully. Fig. 4A shows that the pulmonary lobule structure of mice in the PBS group was intact. An alveolar cavity was clearly visible without exudation, inflammatory cell infiltration and edema in the alveolar septum. After LPS treatment, the mice developed severe acute lung injury symptoms: inflammatory cell infiltration, alveolar wall thickening, massive inflammatory cell exudation in the alveolar cavity, pulmonary hemorrhage, and interstitial edema, which indicate the establishment of the disease model (Fig. 4A). Instillation of LPS into the trachea induces a robust inflammatory reaction within hours to days, which lasts for a certain period of time [52–54]. However, the pathological changes of lung tissues in mice treated with the DEX, PFTU NPs, and PFTU@DEX NPs were improved to different degrees, especially when the PFTU@DEX NPs were administered (Fig. 4A). The experimental data show that the pulmonary delivery exhibited better retention ability in lung [55]. When the NPs reach the lung tissue containing high ROS concentration, the polymers react with ROS, the NPs disintegrate, and the released DEX enhances the therapeutic effect.

In vivo toxicity results show that the main organs including lung, heart, liver, spleen, and kidney had not obvious changes in mice treated with DEX, PFTU NPs, and PFTU@DEX NPs inhalation (Fig. S5A). The serum levels of AST, ALT, BUN, and CRE were normal in the four groups, indicating that the DEX, PFTU NPs, and PFTU@DEX NPs do not induce hepatic or renal injury or failure in 72 h (Fig. S5B).

In severe lung injury, lung capillary permeability increases, resulting in a large amount of extravasation of proteins and other substances. Therefore, total protein concentration in BALF is an important indicator of capillary permeability in lung injury. As shown in Fig. 4C, the DEX, PFTU NPs, and PFTU@DEX NPs treatment all significantly reduced the increased total protein concentration in BALF of mice during acute lung injury, with PFTU@DEX NPs having the greatest degree of remission. Meanwhile, there were abundant infiltration of inflammatory cells (Fig. 4D), especially neutrophils in the BALF during the disease progression. Neutrophils were obtained through a series of gates (Fig. S6). Flow cytometry of inflammatory cells in BALF showed that only alveolar macrophages were present in the BALF of mice in the PBS group, but there were many inflammatory cells in the BALF of mice in the LPS group, more than 80% of which were neutrophils (Fig. 4E and Fig. S6B). However, the number of inflammatory cells and the proportion of neutrophils in the DEX, PFTU NPs, and PFTU@DEX NPs treatment groups were significantly reduced, and the proportion of neutrophils in the PFTU@DEX NPs treatment group decreased the most. Consistent with our results, previous studies show that infiltrated inflammatory cells such as neutrophils, monocytes, macrophages, T cells and B cells will cause immune pathological damage to lung, and also secrete cytokines to induce more infiltration of inflammatory cells, which can indicate the severity of lung inflammation [56–58].

MPO is a specific marker of neutrophil infiltration, indicating inflammatory injury of lung [59]. Immunohistochemical staining of MPO, mainly from neutrophils, also confirmed the therapeutic effect of our PFTU@DEX NPs treatment (Fig. 4F). The extensive infiltration of MPO positive cells, which were stained brown, were

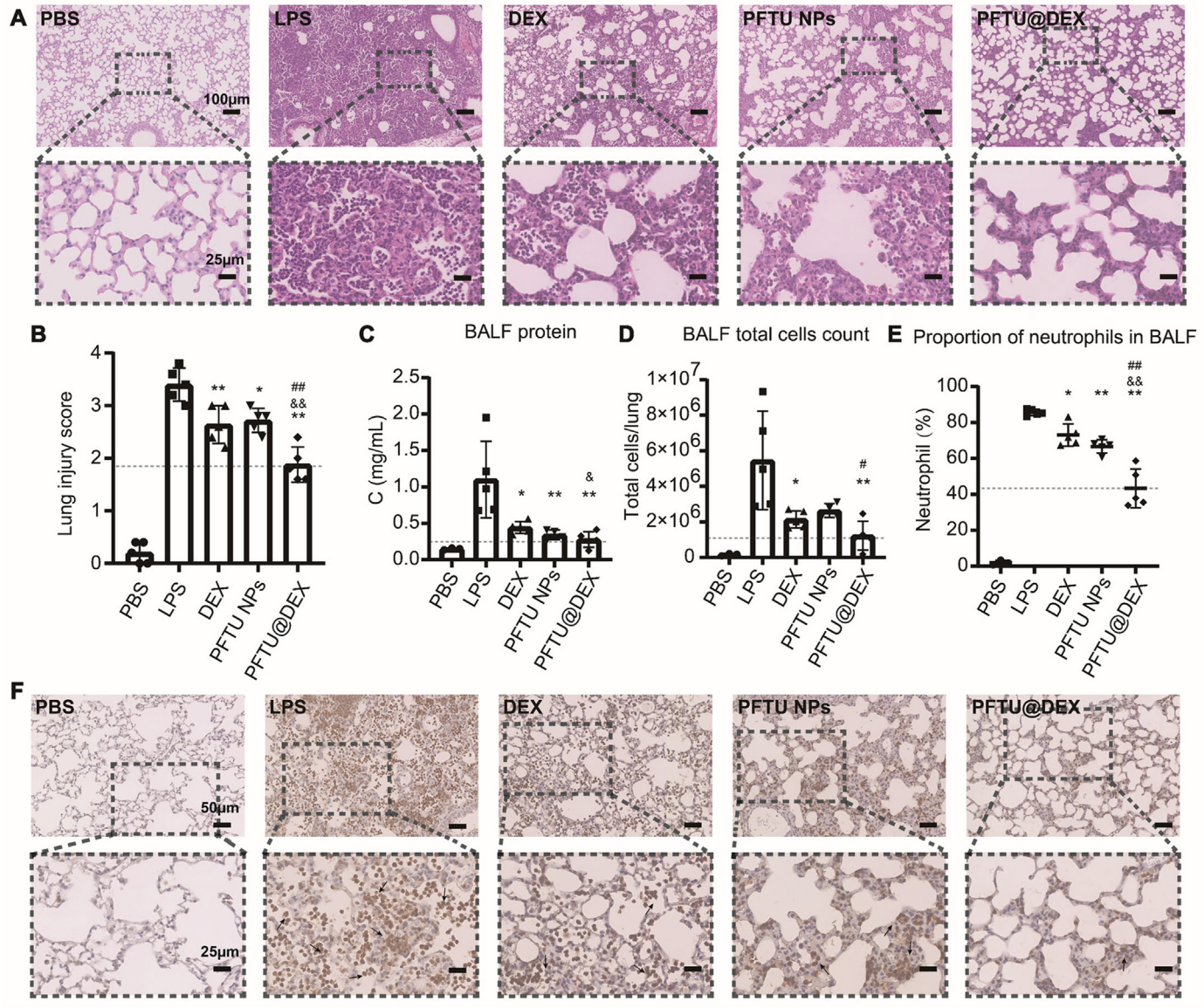

Fig. 4. Inhalation of PFTU@DEX NPs ameliorated LPS-induced ALI at day 3. (A) Hematoxylin and eosin (H&E)-staining images (20×) of lungs. Lower panel shows the higher magnification images (80×) of corresponding samples at the regions marked by black-boxes. (B) Histogram of lung injury scores (n = 5). (C) BALF total protein was determined in ALI mice after treatment with various formulations by BCA kit (n = 3-5). (D) Total cell counts in BALF (n = 3-5) of mice being treated with various formulations. (E) Percentage changes of neutrophils in BALF during ALI with various treatments (n = 3-5). (F) Expression of MPO in mouse lung sections by immunohistochemical staining (40×). Lower panel shows the higher magnification images (80×) of corresponding samples at the regions marked by black-boxes. The black arrows indicate MPO positive cells. The dotted horizontal line represents the mean of PFTU@DEX NPs group. ANOVA followed by Tukey-test. Data are expressed as mean ± SD $^{*}P < 0.05$, $^{**}P < 0.01$ vs LPS group. $^{\&}P < 0.05$, $^{\&\&}P < 0.01$ vs DEX group. $^{\#}P < 0.05$, $^{\#\#}P < 0.01$ vs PFTU NPs group.

tremendously alleviated by the endotracheal intubation atomization of PFTU@DEX NPs.

Taken together, the severe lung injury during ALI was significantly alleviated by administration of the PFTU@DEX NPs.

3.4. Inhibition of inflammatory factors and cell apoptosis

Excessive alveolar epithelial cell apoptosis is the main factor in pathophysiological progression in ALI [60]. The increased production and release of inflammatory mediators such as IFN-γ, TNF-α, IL-6, and ROS could increase cell death by promoting apoptosis [61–63]. Therefore, the suppression of inflammatory cell infiltration, secretion of inflammatory factors, and apoptosis of epithelial cells are vital for the treatment of ALI.

The concentrations of inflammatory factors including IFN-γ, TNF-α, and IL-6 were significantly increased in the BALF and serum of mice treated with LPS, which became lower in the BALF of DEX, PFTU NPs, and PFTU@DEX NPs treatment groups (Fig. 5A, B). The lowest inflammatory factors in alveolar lavage fluid and serum in the PFTU@DEX NPs group validate that the combination of both NPs and DEX modulates the pro-inflammatory cytokine levels effectively.

As determined by the TUNEL staining, the lung cell apoptosis increased significantly after aerosol inhalation of LPS compared with the PBS group (Fig. 5C). Administration of the DEX, PFTU NPs, and PFTU@DEX NPs significantly decreased the phenomenon of apoptosis. Previous research shows that the combination of halofuginone (HF) and DEX has a certain effect on reducing lung fibrosis, inflammation, and alveolar edema in LPS-induced ALI rats [64]. The PFTU@DEX NPs treatment remarkably mitigated the cell apoptosis compared to the LPS, DEX, and PFTU NPs groups. These results indicate that the ROS-responsive-NPs loaded with DEX in-

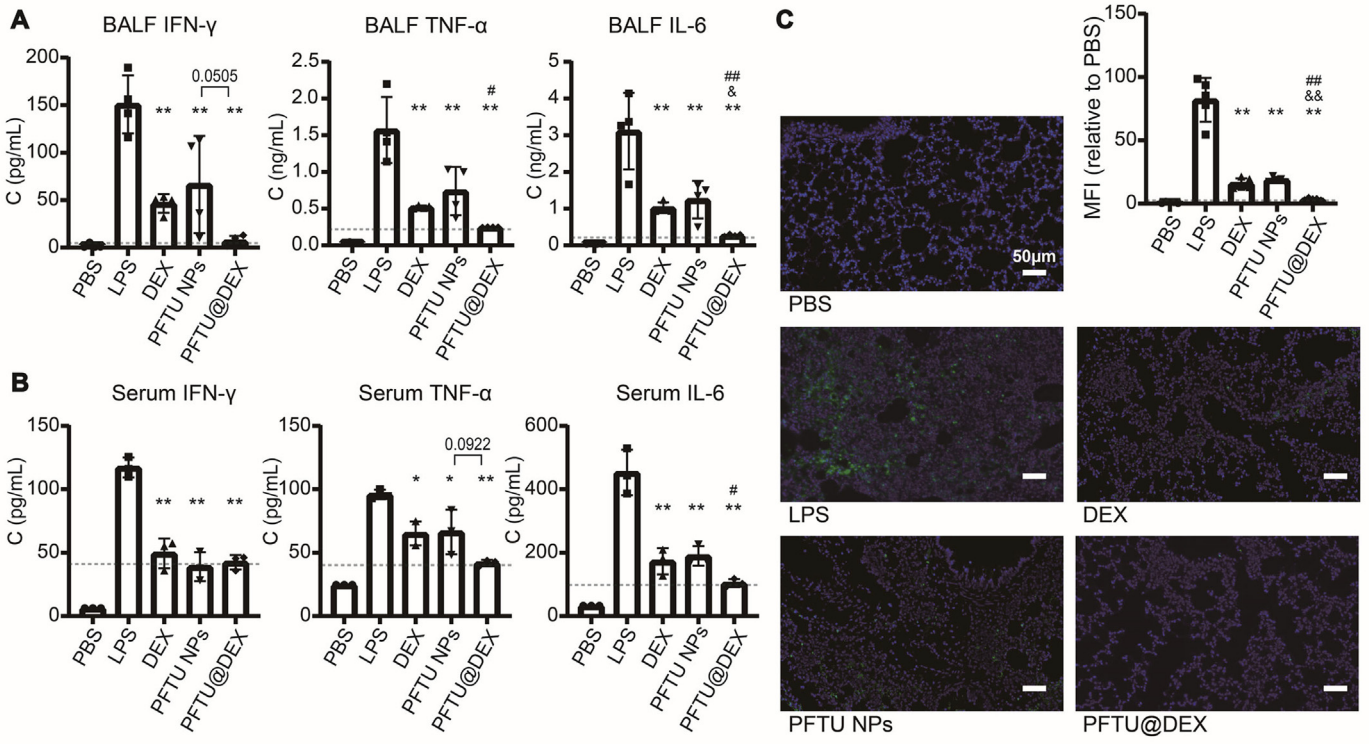

Fig. 5. Inhalation of PFTU@DEX NPs inhibited the inflammatory factors and cell apoptosis. The secretion of IFN-γ, TNF-α and IL-6 in BALF (A) and serum (B) evaluated by LEGENDplex™ multianalyte flow assay (n = 3-4). (C) Cell apoptosis 72 h after LPS inhalation and different treatments in injured area determined by TUNEL staining (n = 5). The dotted horizontal line represents the mean of PFTU@DEX NPs group. ANOVA followed by Tukey-test. Data are expressed as means ± SD. $^{*}P < 0.05$, $^{**}P < 0.01$ vs LPS group. $^{\&}P < 0.05$, $^{\&\&}P < 0.01$ vs DEX group. $^{\#}P < 0.05$, $^{\#\#}P < 0.01$ vs PFTU NPs group.

deed can reduce the early apoptosis of lung cells after ALI, confirming the synergetic effect of NPs and DEX on diminishing lung apoptosis.

3.5. Inhibition of ROS-NLRP3 signaling pathway and M1 macrophages

As the PFTU NPs and PFTU@DEX NPs are ROS scavenging NPs, it is important to measure the ROS levels *in vivo*. The mice were injected with the L012 probe, a ROS-specific bioluminescent probe to evaluate the ROS levels in the different groups (Fig. 6A, B). The relative content of ROS was highest in the LPS group *in vivo* and *ex vivo*, indicating that the inflammation and ROS production were most severe during acute injury. The DEX, PFTU NPs, and PFTU@DEX NPs all had certain ROS-scavenging effects. The PFTU@DEX NPs significantly reduced the local expression of ROS, which was the lowest compared with the DEX and PFTU NPs groups, confirming the best scavenging of local ROS due to their sustainable ROS-clearance effect and loading of DEX.

More and more shreds of evidence indicate that the activation of inflammasome plays a key role in the formation of ALI [65,66]. Previous studies report that the NLRP3 inflammasome in the lung tissue of ALI mice is significantly activated, which mediates the inflammatory damage of the lung tissue, while ROS can mediate the NLRP3 inflammasome activation through the mitochondrial pathway [67–69]. A high level of ROS can lead to the activation of the NLRP3 inflammasome. IL-1β produced by NLRP3 inflammasome activation has a very strong immunomodulatory capacity, and is a key pro-inflammatory factor in initiating inflammatory response [70]. Transient expression of IL-1β alone in the lungs of mice has been reported to cause severe acute lung injury symptoms [71]. Our results show that the LPS stimulation resulted in the increased expression of NLRP3, Caspase1, and IL-1β proteins in the lung tissues compared with the PBS group (Fig. 6C). The free DEX and PFTU NPs reduced slightly the expression of these inflammatory proteins compared to the LPS group. By contrast, the PFTU@DEX NPs had the strongest ability to suppress the expression of NLRP3, Caspase1, and IL-1β. In summary, the PFTU@DEX NPs play a critical role in inhibiting ROS and NLRP3 inflammasome *in vivo*.

Activation of NLRP3 inflammasome can induce more neutrophil infiltration [72], and macrophage activation and polarization into M1 pro-inflammatory phenotype [73]. In the acute stage of ALI, continuous polarization of M1 causes the release of TNF-α, IL-1, and ROS to induce severe inflammatory responses. By contrast, the M2 macrophages are functionally beneficial for inflammatory remission, angiogenesis and tissue repair [74]. Hence, the macrophages were obtained through a series of gates (Fig. S7A). Flow cytometry results show that the proportion of iNOS-expressing macrophages in the lung tissues of LPS-induced acute lung injury mice was significantly increased compared to the PBS group (Fig. 6D, Fig. S7B). The DEX, PFTU NPs, and PFTU@DEX NPs reduced M1 macrophages and increased M2 macrophages. In particular, the PFTU NPs could decrease the proportion of iNOS-positive cells and increase the proportion of Arg-1 positive cells to a certain extent. In summary, the PFTU@DEX NPs show a more significant effect on the inhibition of M1 macrophages and promotion M2 macrophages.

ALI is characterized by inflammatory cell infiltration, uncontrolled inflammatory processes, and oxidative stress. In this study, a modified emulsion method improved the DEX loading to NPs significantly. Meanwhile, the LPS-induced ALI mouse model was also improved compared with the previous oropharyngeal inhalation model. All the results prove that the ROS-responsive NPs can efficiently deliver DEX to infected lungs and enhance their therapeutic effect in the LPS-induced ALI model. Hence, the PFTU@DEX NPs have a potential to be developed further as a safe and effective nanomedicine for the targeted therapy for ALI and ARDS.

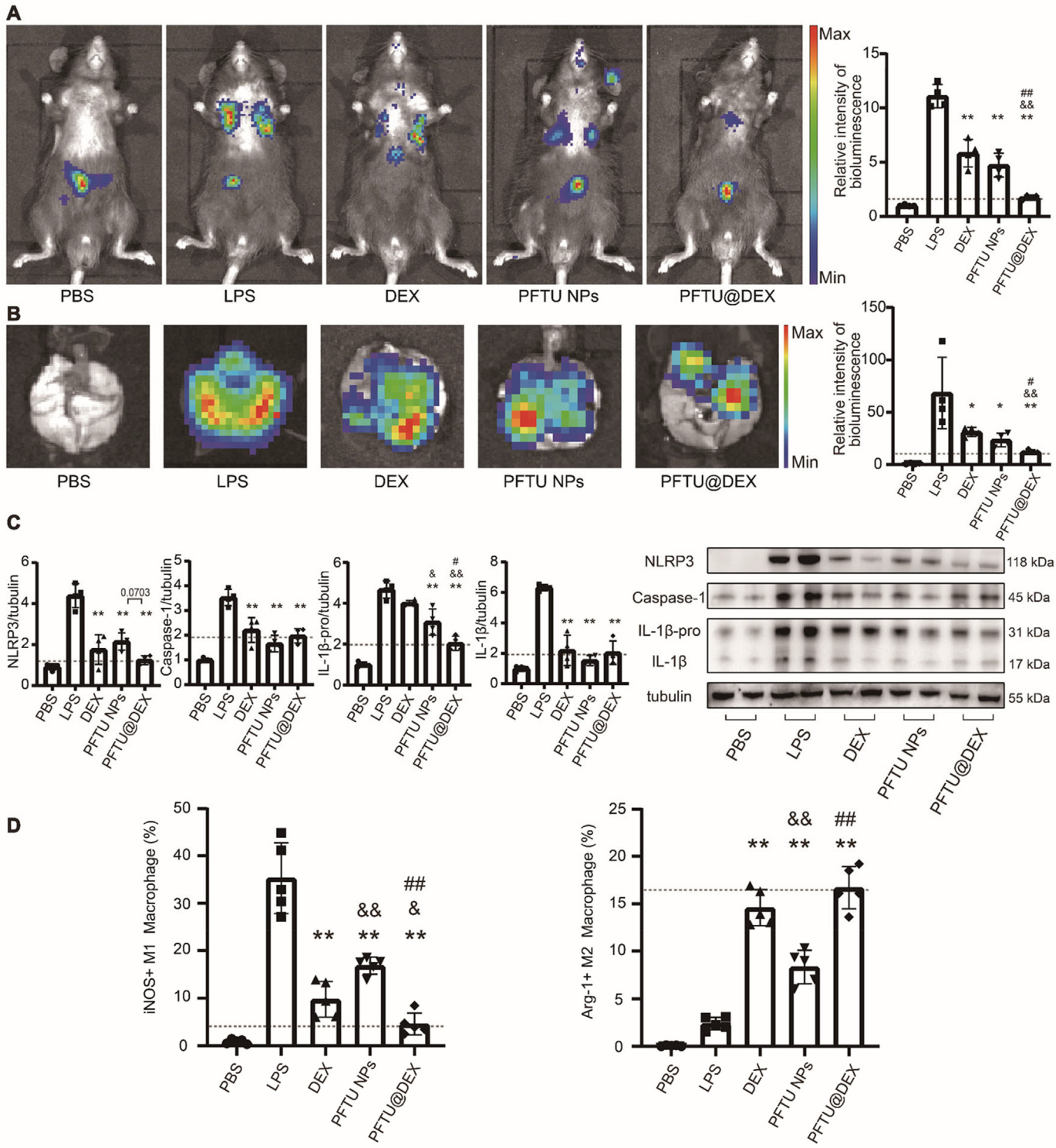

Fig. 6. Inhalation of PFTU@DEX NPs inhibited ROS-NLRP3 signaling pathway and promoted M2-type differentiation of macrophages. Bioluminescence images of mice being injected with L-012 probe (represents the expression of ROS, 50 μg/g) *in vivo* (A) and lung *ex vivo* (B) after different treatments (n = 4). (C) Western blotting of NLRP3, caspase1, IL-1β-pro and IL-1β in lung tissues after treatment with various formulations. The NLRP3, caspase1, IL-1β-pro and IL-1β expression levels are normalized against tubulin (n = 4). (D) Expression of intracellular iNOS (M1 macrophage marker) and Arg-1 (M2 macrophage marker) in lung macrophages after being treated with various formulations analyzed by flow cytometry (n = 5). The dotted horizontal line represents the mean of PFTU@DEX NPs group. ANOVA followed by Tukey-test. Data are expressed as mean ± SD. $^{*}P < 0.05$, $^{**}P < 0.01$ vs LPS group. $^{\&}P < 0.05$, $^{\&\&}P < 0.01$ vs DEX group. $^{\#}P < 0.05$, $^{\#\#}P < 0.01$ vs PFTU NPs group.

4. Conclusions

A ROS-responsive polymer (PFTU) consisting of thioketal bonds was used to prepare NPs with and without the addition of DEX. A modified emulsification method was developed to enhance the loading content of DEX to NPs and tune the size of NPs. The spherical shape PFTU NPs and PFTU@DEX NPs were found non-hemolytic with RBCs. The biocompatible PFTU@DEX NPs degraded after reacting with ROS, and thereby the release of DEX was accelerated. The PFTU@DEX NPs eliminated the excessive ROS and inhibited the activation of the NLRP3 inflammasome, reduced M1 macrophages, and increased M2 macrophages, and thereby reducing the neutrophil infiltration, inhibiting the secretion of proteins and inflammatory factors in lung tissues, and decreasing the lung damage. The PFTU@DEX NPs with good therapeutic potential are expected to exert great advantages in the treatment of lung injury. Moreover, the preparation of NPs by such a method could help reduce the use of costly materials and may decrease the burden of high doses of medications in clinical use.

Finally, the active double bonds on the main chain of the polyurethane (PFTU) allows the grafting of functional substances such as anti-inflammatory drugs, antibiotics and functional molecules by click chemical reactions, which can capture inflammatory factors *in situ*.

Data Availability

The raw/processed data required to reproduce these findings cannot be shared at this time due to technical or time limitations

Declaration of Competing Interest

The authors declare that they have no known competing financial interests or personal relationships that could have appeared to influence the work reported in this paper.

Acknowledgments

This study is financially supported by the Natural Science Foundation of Zhejiang Province (LD21E030001), the National Natural Science Foundation of China (51873188), and Stem Cell and Translational Research, National Key Research and Development Program of China (2020YFA0113003).

Supplementary materials

Supplementary material associated with this article can be found, in the online version, at doi:10.1016/j.actbio.2022.06.024.

References

[1] H. Jin, Z. Zhao, Q. Lan, H. Zhou, Z. Mai, Y. Wang, X. Ding, W. Zhang, J. Pi, C.E. Evans, Nasal delivery of hesperidin/chitosan nanoparticles suppresses cytokine storm syndrome in a mouse model of acute lung injury, Front. Pharmacol. (2021) 1786.
[2] Y. Butt, A. Kurdowska, T.C. Allen, Acute lung injury: a clinical and molecular review, Arch. Pathol. Lab. Med. 140 (4) (2016) 345–350.
[3] Y. Xiong, W. Gao, F. Xia, Y. Sun, L. Sun, L. Wang, S. Ben, S.E. Turvey, H. Yang, Q. Li, Peptide–Gold Nanoparticle Hybrids as Promising Anti-Inflammatory Nanotherapeutics for Acute Lung Injury: in Vivo Efficacy, Biodistribution, and Clearance, Adv. Healthc. Mater. 7 (19) (2018) 1800510.
[4] A. García-Fernández, M. Sancho, V. Bisbal, P. Amorós, M.D. Marcos, M. Orzáez, F. Sancenón, R. Martínez-Máñez, Targeted-lung delivery of dexamethasone using gated mesoporous silica nanoparticles. A new therapeutic approach for acute lung injury treatment, J. Controlled Release 337 (2021) 14–26.
[5] W. Muhammad, Z. Zhai, S. Wang, C. Gao, Inflammation-modulating nanoparticles for pneumonia therapy, Wiley Interdiscip. Rev. Nanomed. Nanobiotechnol. (2021) e1763.
[6] H. Zhang, H. Xiong, W. Ahmed, Y. Yao, S. Wang, C. Fan, C. Gao, Reactive oxygen species-responsive and scavenging polyurethane nanoparticles for treatment of osteoarthritis in vivo, Chem. Eng. J. 409 (2021) 128147.
[7] X. Liu, Z. Chen, The pathophysiological role of mitochondrial oxidative stress in lung diseases, J. Transl. Med. 15 (1) (2017) 1–13.
[8] H. Zhou, E.K. Fan, J. Fan, Cell—cell interaction mechanisms in acute lung injury, Shock 55 (2) (2021) 167.
[9] L. Zuo, D. Wijegunawardana, Redox role of ROS and Inflammation in pulmonary diseases, Lung Inflamm. Health Dis. II (2021) 187–204.
[10] M. Kellner, S. Noonepalle, Q. Lu, A. Srivastava, E. Zemskov, S.M. Black, in: ROS signaling in the pathogenesis of acute lung injury (ALI) and acute respiratory distress syndrome (ARDS), Pulmonary Vasculature Redox Signaling in Health and Disease, Springer, 2017, pp. 105–137.
[11] L. Chen, L. Zhao, C. Zhang, Z. Lan, Protective effect of p-cymene on lipopolysaccharide-induced acute lung injury in mice, Inflammation 37 (2) (2014) 358–364.
[12] M.D. Howard, C.F. Greineder, E.D. Hood, V.R. Muzykantov, Endothelial targeting of liposomes encapsulating SOD/catalase mimetic EUK-134 alleviates acute pulmonary inflammation, J. Controlled Release 177 (2014) 34–41.
[13] R. Zhu, T. Yan, Y. Feng, Y. Liu, H. Cao, G. Peng, Y. Yang, Z. Xu, J. Liu, W. Hou, Mesenchymal stem cell treatment improves outcome of COVID-19 patients via multiple immunomodulatory mechanisms, Cell Res. (2021) 1–19.
[14] P.T. Goud, D. Bai, H.M. Abu-Soud, A Multiple-Hit Hypothesis Involving Reactive Oxygen Species and Myeloperoxidase Explains Clinical Deterioration and Fatality in COVID-19, Int. J. Biol. Sci. 17 (1) (2021) 62.
[15] R. Cecchini, A.L. Cecchini, SARS-CoV-2 infection pathogenesis is related to oxidative stress as a response to aggression, Med. Hypotheses 143 (2020) 110102.
[16] Y. Yao, H. Zhang, Z. Wang, J. Ding, S. Wang, B. Huang, S. Ke, C. Gao, Reactive oxygen species (ROS)-responsive biomaterials mediate tissue microenvironments and tissue regeneration, J. Mater. Chem. B 7 (33) (2019) 5019–5037.
[17] W.-H. Chen, Q.-W. Chen, Q. Chen, C. Cui, S. Duan, Y. Kang, Y. Liu, Y. Liu, W. Muhammad, S. Shao, Biomedical polymers: synthesis, properties, and applications, Sci. China Chem. (2022) 1–66.
[18] J. Liu, Y. Li, S. Chen, Y. Lin, H. Lai, B. Chen, T. Chen, Biomedical application of reactive oxygen species–responsive nanocarriers in cancer, inflammation, and neurodegenerative diseases, Front. Chem. 8 (2020).
[19] M. Doroudian, M.H. Azhdari, N. Goodarzi, D. O'Sullivan, S.C. Donnelly, Smart Nanotherapeutics and Lung Cancer, Pharmaceutics 13 (11) (2021) 1972.
[20] Y. Wang, Q. Yuan, W. Feng, W. Pu, J. Ding, H. Zhang, X. Li, B. Yang, Q. Dai, L. Cheng, Targeted delivery of antibiotics to the infected pulmonary tissues using ROS-responsive nanoparticles, J. Nanobiotechnol. 17 (1) (2019) 1–16.
[21] Y. Zhang, H. Zhang, Z. Mao, C. Gao, ROS-responsive nanoparticles for suppressing the cytotoxicity and immunogenicity caused by PM2. 5 particulates, Biomacromolecules 20 (4) (2019) 1777–1788.
[22] Y. Liu, G. Yang, S. Jin, L. Xu, C.X. Zhao, Development of High-Drug-Loading Nanoparticles, ChemPlusChem 85 (9) (2020) 2143–2157.
[23] Y. Liu, G. Yang, T. Baby, D. Chen, D.A. Weitz, C.X. Zhao, Stable polymer nanoparticles with exceptionally high drug loading by sequential nanoprecipitation, Angew. Chem. 132 (12) (2020) 4750–4758.
[24] K. Cai, X. He, Z. Song, Q. Yin, Y. Zhang, F.M. Uckun, C. Jiang, J. Cheng, Dimeric drug polymeric nanoparticles with exceptionally high drug loading and quantitative loading efficiency, J. Am. Chem. Soc. 137 (10) (2015) 3458–3461.
[25] W.S. Cheow, K. Hadinoto, Self-assembled amorphous drug–polyelectrolyte nanoparticle complex with enhanced dissolution rate and saturation solubility, J. Colloid Interface Sci. 367 (1) (2012) 518–526.
[26] S.F. Chow, K.Y. Wan, K.K. Cheng, K.W. Wong, C.C. Sun, L. Baum, A.H.L. Chow, Development of highly stabilized curcumin nanoparticles by flash nanoprecipitation and lyophilization, Eur. J. Pharm. Biopharm. 94 (2015) 436–449.
[27] Z. Zhu, Y. Li, X. Li, R. Li, Z. Jia, B. Liu, W. Guo, W. Wu, X. Jiang, Paclitaxel-loaded poly (N-vinylpyrrolidone)-b-poly (ε-caprolactone) nanoparticles: preparation and antitumor activity in vivo, J. Controlled Release 142 (3) (2010) 438–446.
[28] F. Liu, J.-Y. Park, Y. Zhang, C. Conwell, Y. Liu, S.R. Bathula, L. Huang, Targeted cancer therapy with novel high drug-loading nanocrystals, J. Pharm. Sci. 99 (8) (2010) 3542–3551.
[29] J. Xie, Y. Yao, S. Wang, L. Fan, J. Ding, Y. Gao, S. Li, L. Shen, Y. Zhu, C. Gao, Alleviating Oxidative Injury of Myocardial Infarction by a Fibrous Polyurethane Patch with Condensed ROS-scavenging Backbone Units, Adv. Healthc. Mater. (2021) 2101855.
[30] J.W. Yang, B. Mao, R.J. Tao, L.C. Fan, H.W. Lu, B.X. Ge, J.F. Xu, Corticosteroids alleviate lipopolysaccharide-induced inflammation and lung injury via inhibiting NLRP3-inflammasome activation, J. Cell. Mol. Med. 24 (21) (2020) 12716–12725.
[31] N.O. Al-Harbi, F. Imam, M.M. Al-Harbi, M.A. Ansari, K.M. Zoheir, H.M. Korashy, M.M. Sayed-Ahmed, S.M. Attia, O.A. Shabanah, S.F. Ahmad, Dexamethasone attenuates LPS-induced acute lung injury through inhibition of NF-κB, COX-2, and pro-inflammatory mediators, Immunol. Invest. 45 (4) (2016) 349–369.
[32] R. Zhang, R. Liu, C. Liu, L. Pan, Y. Qi, J. Cheng, J. Guo, Y. Jia, J. Ding, J. Zhang, A pH/ROS dual-responsive and targeting nanotherapy for vascular inflammatory diseases, Biomaterials 230 (2020) 119605.
[33] J. Liu, P. Li, J. Zhu, F. Lin, J. Zhou, B. Feng, X. Sheng, X. Shi, Q. Pan, J. Yu, Mesenchymal stem cell-mediated immunomodulation of recruited mononuclear phagocytes during acute lung injury: a high-dimensional analysis study, Theranostics 11 (5) (2021) 2232.
[34] J. Zhu, B. Feng, Y. Xu, W. Chen, X. Sheng, X. Feng, X. Shi, J. Liu, Q. Pan, J. Yu, Mesenchymal stem cells alleviate LPS-induced acute lung injury by inhibiting the proinflammatory function of Ly6C+ CD8+ T cells, Cell Death. Dis. 11 (10) (2020) 1–11.

[35] B. Feng, J. Zhu, Y. Xu, W. Chen, X. Sheng, X. Feng, X. Shi, J. Liu, Q. Pan, J. Yang, Immunosuppressive effects of mesenchymal stem cells on lung B cell gene expression in LPS-induced acute lung injury, Stem Cell Res. Therapy 11 (1) (2020) 1–9.
[36] H.-H. Yang, J.-X. Duan, S.-K. Liu, J.-B. Xiong, X.-X. Guan, W.-J. Zhong, C.-C. Sun, C.-Y. Zhang, X.-Q. Luo, Y.-F. Zhang, A COX-2/sEH dual inhibitor PTUPB alleviates lipopolysaccharide-induced acute lung injury in mice by inhibiting NLRP3 inflammasome activation, Theranostics 10 (11) (2020) 4749.
[37] S. Shen, Y. Wu, Y. Liu, D. Wu, High drug-loading nanomedicines: progress, current status, and prospects, Int. J. Nanomed. 12 (2017) 4085.
[38] V. Mishra, P. Nayak, N. Yadav, M. Singh, M.M. Tambuwala, A.A. Aljabali, Orally administered self-emulsifying drug delivery system in disease management: Advancement and patents, Expert Opin. Drug Deliv. 18 (3) (2021) 315–332.
[39] Y. Yao, J. Ding, Z. Wang, H. Zhang, J. Xie, Y. Wang, L. Hong, Z. Mao, J. Gao, C. Gao, ROS-responsive polyurethane fibrous patches loaded with methylprednisolone (MP) for restoring structures and functions of infarcted myocardium in vivo, Biomaterials 232 (2020) 119726.
[40] B. Chen, Y. Zhang, R. Ran, B. Wang, F. Qin, T. Zhang, G. Wan, H. Chen, Y. Wang, Reactive oxygen species-responsive nanoparticles based on a thioketal-containing poly (β-amino ester) for combining photothermal/photodynamic therapy and chemotherapy, Polym. Chem. 10 (34) (2019) 4746–4757.
[41] Z. Zhai, W. Ouyang, Y. Yao, Y. Zhang, H. Zhang, F. Xu, C. Gao, Dexamethasone-loaded ROS-responsive poly (thioketal) nanoparticles suppress inflammation and oxidative stress of acute lung injury, Bioactive Mater. (2022).
[42] M.A. Dobrovolskaia, J.D. Clogston, B.W. Neun, J.B. Hall, A.K. Patri, S.E. McNeil, Method for analysis of nanoparticle hemolytic properties in vitro, Nano Lett. 8 (8) (2008) 2180–2187.
[43] H.-Y. Liu, L. Du, Y.-T. Zhao, W.-Q. Tian, In vitro hemocompatibility and cytotoxicity evaluation of halloysite nanotubes for biomedical application, J. Nanomaterials (2015) 2015.
[44] Z.-jj. Wang, C.-yy. Liu, Z.-yy. Qian, D.-ww. Gao, X.-mm. Guo, Anticoagulant chitosan nanoparticles: synthesis, characterization and biological safety, Chin. J. Tissue Eng. Res. 19 (47) (2015) 7655.
[45] R. van Lith, E.K. Gregory, J. Yang, M.R. Kibbe, G.A. Ameer, Engineering biodegradable polyester elastomers with antioxidant properties to attenuate oxidative stress in tissues, Biomaterials 35 (28) (2014) 8113–8122.
[46] Z.E. Pápay, A. Kósa, B. Böddi, Z. Merchant, I.Y. Saleem, M.G. Zariwala, I. Klebovich, S. Somavarapu, I. Antal, Study on the pulmonary delivery system of apigenin-loaded albumin nanocarriers with antioxidant activity, J. Aerosol Med. Pulmonary Drug Deliv. 30 (4) (2017) 274–288.
[47] Y. Yao, X.-H. Xu, L. Jin, Macrophage polarization in physiological and pathological pregnancy, Front. Immunol. 10 (2019) 792.
[48] R.H. Patil, M.N. Kumar, K.K. Kumar, R. Nagesh, K. Kavya, R. Babu, G.T. Ramesh, S.C. Sharma, Dexamethasone inhibits inflammatory response via down regulation of AP-1 transcription factor in human lung epithelial cells, Gene 645 (2018) 85–94.
[49] H. Chen, C. Bai, X. Wang, The value of the lipopolysaccharide-induced acute lung injury model in respiratory medicine, Expert Rev. Respir. Med. 4 (6) (2010) 773–783.
[50] M.E. Ali, J.T. McConville, A. Lamprecht, Pulmonary delivery of anti-inflammatory agents, Expert Opin. Drug Deliv. 12 (6) (2015) 929–945.
[51] H.L. Dugasa, R.O. Williams III, Nanotechnology for Pulmonary and Nasal Drug Delivery, Nanotechnology and Drug Delivery, Volume Two, Nano-Eng. Strat. Nanomed. Against Severe Dis. 102 (2016).
[52] F.R. D'Alessio, K. Tsushima, N.R. Aggarwal, E.E. West, M.H. Willett, M.F. Britos, M.R. Pipeling, R.G. Brower, R.M. Tuder, J.F. McDyer, CD4+ CD25+ Foxp3+ Tregs resolve experimental lung injury in mice and are present in humans with acute lung injury, J. Clin. Invest. 119 (10) (2009) 2898–2913.
[53] D. Rittirsch, M.A. Flierl, D.E. Day, B.A. Nadeau, S.R. McGuire, L.M. Hoesel, K. Ipaktchi, F.S. Zetoune, J.V. Sarma, L. Leng, Acute lung injury induced by lipopolysaccharide is independent of complement activation, J. Immunol. 180 (11) (2008) 7664–7672.
[54] Y. Yu, L. Jing, X. Zhang, C. Gao, Simvastatin attenuates acute lung injury via regulating CDC42-PAK4 and endothelial microparticles, Shock 47 (3) (2017) 378–384.
[55] Q.T. Jin, W.J. Zhu, J.F. Zhu, J.J. Zhu, J.J. Shen, Z. Liu, Y. Yang, Q. Chen, Nanoparticle-Mediated Delivery of Inhaled Immunotherapeutics for Treating Lung Metastasis, Adv. Mater. 33 (7) (2021).
[56] J. Liu, P. Li, J. Zhu, F. Lin, J. Zhou, B. Feng, X. Sheng, X. Shi, Q. Pan, J. Yu, J. Gao, L. Li, H. Cao, Mesenchymal stem cell-mediated immunomodulation of recruited mononuclear phagocytes during acute lung injury: a high-dimensional analysis study, Theranostics 11 (5) (2021) 2232–2246.
[57] J. Zhu, B. Feng, Y. Xu, W. Chen, X. Sheng, X. Feng, X. Shi, J. Liu, Q. Pan, J. Yu, L. Li, H. Cao, Mesenchymal stem cells alleviate LPS-induced acute lung injury by inhibiting the proinflammatory function of Ly6C(+) CD8(+) T cells, Cell Death Dis. 11 (10) (2020) 829.
[58] B. Feng, J. Zhu, Y. Xu, W. Chen, X. Sheng, X. Feng, X. Shi, J. Liu, Q. Pan, J. Yang, J. Yu, L. Li, H. Cao, Immunosuppressive effects of mesenchymal stem cells on lung B cell gene expression in LPS-induced acute lung injury, Stem Cell Res. Ther. 11 (1) (2020) 418.
[59] Y. Nie, Z. Wang, G. Chai, Y. Xiong, B. Li, H. Zhang, R. Xin, X. Qian, Z. Tang, J. Wu, P. Zhao, Dehydrocostus Lactone Suppresses LPS-induced Acute Lung Injury and Macrophage Activation through NF-kappaB Signaling Pathway Mediated by p38 MAPK and Akt, Molecules 24 (8) (2019).
[60] C.C. Nan, N. Zhang, K.C.P. Cheung, H.D. Zhang, W. Li, C.Y. Hong, H.S. Chen, X.Y. Liu, N. Li, L. Cheng, Knockdown of lncRNA MALAT1 Alleviates LPS-Induced Acute Lung Injury via Inhibiting Apoptosis Through the miR-194-5p/FOXP2 Axis, Front. Cell Dev. Biol. 8 (2020) 586869.
[61] E.A. Kang, H.I. Choi, S.W. Hong, S. Kang, H.Y. Jegal, E.W. Choi, B.S. Park, J.S. Kim, Extracellular Vesicles Derived from Kefir Grain Lactobacillus Ameliorate Intestinal Inflammation via Regulation of Proinflammatory Pathway and Tight Junction Integrity, Biomedicines 8 (11) (2020).
[62] R. Johnson, P.V. Dludla, C.J. Muller, B. Huisamen, M.F. Essop, J. Louw, The Transcription Profile Unveils the Cardioprotective Effect of Aspalathin against Lipid Toxicity in an In Vitro H9c2 Model, Molecules 22 (2) (2017).
[63] L. Shojaie, A. Iorga, L. Dara, Cell Death in Liver Diseases: a Review, Int. J. Mol. Sci. 21 (24) (2020).
[64] H.L. Du, A.D. Zhai, H. Yu, Synergistic effect of halofuginone and dexamethasone on LPSinduced acute lung injury in type II alveolar epithelial cells and a rat model, Mol. Med. Rep. 21 (2) (2020) 927–935.
[65] T. Dolinay, Y.S. Kim, J. Howrylak, G.M. Hunninghake, C.H. An, L. Fredenburgh, A.F. Massaro, A. Rogers, L. Gazourian, K. Nakahira, J.A. Haspel, R. Landazury, S. Eppanapally, J.D. Christie, N.J. Meyer, L.B. Ware, D.C. Christiani, S.W. Ryter, R.M. Baron, A.M. Choi, Inflammasome-regulated cytokines are critical mediators of acute lung injury, Am. J. Respir. Crit. Care Med. 185 (11) (2012) 1225–1234.
[66] M. Sauler, I.S. Bazan, P.J. Lee, Cell Death in the Lung: the Apoptosis-Necroptosis Axis, Annu. Rev. Physiol. 81 (2019) 375–402.
[67] N. Yin, Z. Peng, B. Li, J. Xia, Z. Wang, J. Yuan, L. Fang, X. Lu, Isoflurane attenuates lipopolysaccharide-induced acute lung injury by inhibiting ROS-mediated NLRP3 inflammasome activation, Am. J. Transl. Res. 8 (5) (2016) 2033–2046.
[68] J. Chen, S. Wang, R. Fu, M. Zhou, T. Zhang, W. Pan, N. Yang, Y. Huang, RIP3 dependent NLRP3 inflammasome activation is implicated in acute lung injury in mice, J. Transl. Med. 16 (1) (2018) 233.
[69] K. Weber, J.D. Schilling, Lysosomes integrate metabolic-inflammatory cross-talk in primary macrophage inflammasome activation, J. Biol. Chem. 289 (13) (2014) 9158–9171.
[70] Y. Xue, H.D. Du, D. Tang, D. Zhang, J. Zhou, C.W. Zhai, C.C. Yuan, C.Y. Hsueh, S.J. Li, Y. Heng, L. Tao, L.M. Lu, Correlation Between the NLRP3 Inflammasome and the Prognosis of Patients With LSCC, Front. Oncol. 9 (2019) 588.
[71] H.A. Chapman, Epithelial-mesenchymal interactions in pulmonary fibrosis, Annu. Rev. Physiol. 73 (2011) 413–435.
[72] Y. Peng, Q. Wu, H. Tang, J. Chen, Q. Wu, X. Yuan, S. Xiong, Y. Ye, H. Lv, NLRP3 Regulated CXCL12 Expression in Acute Neutrophilic Lung Injury, J. Inflamm. Res. 13 (2020) 377–386.
[73] J. Zhang, X. Liu, C. Wan, Y. Liu, Y. Wang, C. Meng, Y. Zhang, C. Jiang, NLRP3 inflammasome mediates M1 macrophage polarization and IL-1beta production in inflammatory root resorption, J. Clin. Periodontol. 47 (4) (2020) 451–460.
[74] X. Chen, J. Tang, W. Shuai, J. Meng, J. Feng, Z. Han, Macrophage polarization and its role in the pathogenesis of acute lung injury/acute respiratory distress syndrome, Inflamm. Res. 69 (9) (2020) 883–895.